

Electrical conductivity, mechanical stability, antibacterial and anticancer activities of ethyl cellulose-tin(II) hydrogen phosphate

Tanvir Arfin^{1*}, Faruq Mohammad^{2*}

¹*Environmental Materials Division, CSIR-National Environmental Engineering Research Institute (CSIR-NEERI), Nehru Marg, Nagpur 440020, India*

²*Institute of Advanced Technology, Universiti Putra Malaysia, Serdang, Selangor 43400, Malaysia*

*Corresponding author. Tel: (+60) 1-73518716; E-mail: t_arfin@neeri.res.in (T. Arfin); faruq_m@upm.edu.my (F. Mohammad)

Received: 12 May 2015, Revised: 10 October 2015 and Accepted: 30 October 2015

ABSTRACT

In the present study, a very prominent cost effective sol-gel method was used to amalgamate the ethyl cellulose-tin(II) hydrogen phosphate (EC-SnHPO₄), an organic-inorganic composite material with certain acidic condition practiced in a conductivity system. The physical characterization of the material was described by the UV-Vis and FTIR study. The different monovalent electrolytes such as KCl (aq) and NaCl (aq) at diverse temperature range was employed to measure the conductivity of EC-SnHPO₄ and also for the concentration to explore between affinity of conductivity and electrochemical properties of the material. From the study, the conductivity was established to be less for K⁺ than Na⁺. For such process in addition, the different parameters such as ionization potential, oscillator strength, transition dipole moment, resonance energy, and transition energy were investigated. Finally, the anticancer effect against the MCF-7 breast cancer cell line and the antibacterial activity against two different bacterial strains show the potential pharmacological activity of the EC-SnHPO₄ towards medical applications. Copyright © 2015 VBRI Press.

Keywords: Tin (II) hydrogen phosphate; conductivity; ionization potential; transition energy; antibacterial activity.

Introduction

The organic-inorganic nanocomposites are generally refer to multiphase materials where one of the constituent phases is found to have at least one dimension in a nanoscale range [1, 2]. The design and creation of new nanocomposites have been authorized by new technical innovations and the structure with unrivalled flexibility, qualitative improvements in their physical property imparts various important aspects in industrial product development. The multifunctional organic-inorganic composites with increased mechanical, electrical, optical, thermal or magnetic properties are approached by nanoscale fillers in organic-inorganic materials which is an opted fact [3, 4]. With this aspect, ethyl cellulose (EC) was extensively used as a dissolution rate controlling polymer in sustained-release dosage forms which is quite complementary [5]. EC is a non-toxic, stable, easily compressible, passive, hydrophobic polymer and hence frequently employed for the preparation of pharmaceutical dosage forms [6]. The film coated tablets, microspheres, microcapsules and matrix tablets extensively include the properties of EC sustained release products for both soluble and poorly soluble drugs that have been reported so far [7]. EC is used for

microencapsulation of different pharmaceutical products to keep in a steady state from the unwanted interactions where it is used as a polymeric coating material, to control the release in oral preparations, in transdermal films and patches (a pharmaceutically active aqueous latex dispersion), and also as a particle emulsion stabilizer [8].

Tin hydrogen phosphate (SnHPO₄) is greatly of biological importance as it is having a peculiar property that it is produced in the reaction lying between SnF₂ and dental enamel below the pH 2 [9]. Yellin and Cilley suggested from the infrared and Raman spectra of SnHPO₄ that the compound is dimeric and contains a novel, linear Sn-O-Sn bond in between them [10]. Klement and Haselbeck gave the confirmation of the presence of one-half molecule of water in each molecule of SnHPO₄ [11]. In 1971, Berndt and Lamberg concluded the structure of SnHPO₄ from their experiments [12]. This determination was repeated many times for various reasons such as (a) the accuracy of atomic parameters in the earlier structure was not sufficient to allow a clear pictoration of tin coordination and it also did not resolve the questions about a linear Sn-O-Sn bond or about lone-pair distortions common to Sn(II) compounds [13, 14] (b) it was also done to prescribe valid comparison between the structures of SnHPO₄ and SnHPO₃, as it was noticed to workout both for copper radiation and no absorption corrections were accompanied.

Ciley studied the solubility of the sparingly soluble $\text{SnHPO}_4 \cdot 0.5\text{H}_2\text{O}$ as a function of orthophosphate concentration in the range 3×10^{-4} - 0.09M by the reaction between Sn^{2+} and PO_4^{3-} ions at 25°C in 0.2 M NaClO_4 (at a constant pH of 2.48) [15].

Gnusin [16] and Zabolotsky and Nikonenko [17] projected a model with a combination of gel and integral phases with volume fractions and, respectively. The integral phase generally represents the inner parts of meso/microscopes (voids/cavities), whereas the gel phase represents the electro neutral nanoporous medium, which basically consists of fixed and mobile ions, water and polymer matrix [18]. The concentration-dependent properties such as conductivity, diffusion permeability, and counter-ion transport are in accordance with the micro heterogeneous structure of the material matrix [19]. It is generally found that the dynamic studies on the electrical conductance of the solutions are corresponding to the investigation of solvation and electro-transport properties of the constituent ions that are present in the solution. Such properties of solution are dependent on both the characteristics of ionic radius and also the degree of ionic hydration [20, 21].

The biomaterials (such as Ag, Au, Zn, Fe, Cu, chitosan, polyethylene glycol, polylactic acid glutamic acid etc) have become the part of human healthcare since from ancient periods due to their nontoxic and efficient nature to be applicable for the diagnosis and treatment of many different diseases related to cancer, cardiovascular, brain, lung and liver, to mention some. The enhancement and utility factors have made the use of biomaterial as multipurpose materials and vast developments have been seen towards their function as well. Despite the developments achieved towards the function and efficiency of the bio/nanocomposites, there has always been a demand for the development of novel materials with enhanced properties of stability under various pHs, time and biological media and that are available for economical price. Similarly, some of the diagnosing materials composed of Au, Ag, Zn and Ti are expensive and are not accessible for all. Hence in the present paper, more attention is levied for the investigation of a non-expensive, non-toxic and efficient nanocomposite material with agitated properties to be applicable in biomedical and pharmaceutical applications.

Based on these facts, the objective of the present study is aimed to improve the possible interactions and characteristic relation between EC and SnHPO_4 . For that, the composite of EC- SnHPO_4 (1:3 wt/wt ratio) was synthesized by sol-gel method with various electrolytes (1:1 ratio) at a range of temperatures and concentrations. By relating the relationship of the square root of electrolyte concentration enormously at the different range of temperature was responsible for increasing the value of material in a non-linear way which showed an exclusive inhibitory outcome irrespective of the bacterial culture such as gram positive and gram negative bacteria. The objective of this EC and Sn-mediated process is to provide less expensive, high mechanical, chemical, and thermal stabilities. It is expected that the formed nanocomposite material to be suited for the expectation of the market in the present and future for improving the facilities related to human health.

Experimental

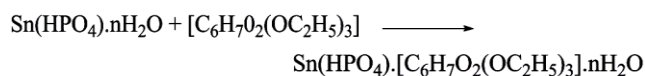
Synthesis of EC-Sn(II)HPO₄ composite

First, Sn(II)HPO_4 precipitates were synthesized by mixing 0.2 M tin(II) chloride (99 %, S.D. Fine-Chem Ltd) with 0.2 M dipotassium hydrogen orthophosphate (98 %, S.D. Fine-Chem Ltd) solution to yield light white precipitates. The pH of the mixture was maintained at 1.0 by the addition of dilute HCl (35.40 %, S.D. Fine-Chem Ltd) on constant stirring and the precipitates left were kept for 24 h at room temperature [22]. The supernatant was separated by centrifugation and the precipitate was well washed with deionized water to remove free electrolyte, and dried at 80 °C and grounded to fine powder with the help of a mortar and pestle, and the powder was sieved using an 85 µm sieve. The tentative chemical formula of the formed product is given below:



In the following step, Sn(II)HPO_4 and EC powders were mixed thoroughly by using mortar and pestle and then the formed mixture was placed in an hot air oven at 80 °C for 1 h [23]. The EC- SnHPO_4 composite prepared by implanting 25 % EC with that of Sn(II)HPO_4 found to exhibit the highest mechanical stability and finally giving out to be the productive and reproducible results. However, the composite that contained greater amounts (>25 %) of EC was not effective enough to give reproducible results whereas the one with lesser amounts (< 25 %) is found unstable. The tablet form of the composite was prepared by compressing the powder using a Tablet compression (Mini press 1 station, Rimek).

The following tentative structure is proposed:



where, 'n' represents the number of hydration water molecules.

Conductivity measurements

The test cells that were used for the electrochemical measurements are very similar to as described elsewhere [24]. With the help of de-ionised water, the different electrolyte solutions (KCl and NaCl) of various concentrations were prepared. In order to minimize concentration-polarization at the material surfaces, a magnetic stirrer was placed at the bottom of each half-cell and its speed was 500 rpm [25]. The solution pH was normally in the range of 5.5-6. The conductivity measurements were carried by adopting one of the qualitative methods as followed by in the temperature range $(5 \pm 50) \pm 0.2$ °C [26]. The material conductivity was observed by utilizing an auto ranging digital conductivity meter (Model No.EQ-667, Equip-Tronics). For each sample, three different measurements were taken and the mean of all these values was considered as the resultant conductivity.

Spectroscopic measurements

The UV-Vis spectrum was recorded by using a UV-1800 spectrophotometer (Shimadzu) and the de-ionised methanol, water were used as solvents for the reference and the composite material respectively. The FTIR spectrum of the EC-SnHPO₄ composite was recorded by using an Alpha-FTIR spectroscopy (Bruker). The sample spectrum obtained by taking out an average of 200 scans between 4000 and 600 cm⁻¹ with a resolution of 4 cm⁻¹ which was corrected at the background spectrum.

Measurement of antibacterial activity

By employing the disc diffusion method, the antibacterial activity of EC-SnHPO₄ was analyzed *in vitro* using gram positive bacteria of *Staphylococcus aureus* (MSSA-22) and gram negative bacteria of *Escherichia coli* (K-12) [27-28]. The testing strains were cultured in nutrient broth comprising of Lab-Lemco powder 0.1 % (w/v), yeast extract 0.2 % (w/v), peptone 0.5 % (w/v), and sodium chloride 5 % (w/v). The bacteria was cultured on Mueller Hinton Agar consists of meat infusion 30 % (w/v); casein hydrolysate 1.75 % (w/v); starch 0.15 % (w/v); agar-agar 1.7 % (w/v).

The screening for antibacterial activity was done by employing sterile discs (5 mm), and these disks were previously soaked in 0.2 M concentration of the test complex (EC-SnHPO₄) and then dried at 70 °C for about 6 h. The tested strains were incubated and made active at 37 °C for 24 h in an inoculation into nutrient broth. Inoculums containing 10⁷-10⁸ CFU of bacterial cells were spread on Mueller-Hinton Agar plates of 100 µL inoculum for each plating. The discs that was soaked with EC-SnHPO₄ composite were inserted on the inoculated agar by slight press and incubated at 37 °C for 24 h. Tetracycline (30 µg/disk, Hi-Media) was used as the control measurements and the inhibition zone was measured after 24 h. All the experiments were repeated 3 times and the values shown are the mean ± SD of all the experiments.

Investigation of anticancer effect

For the investigation of the anticancer effect of EC-SnHPO₄ composite, the MCF-7 human breast cancer cells (from ATCC) were selected. For the treatments, the cells were grown in Dulbecco's Modified Eagle's Medium (DMEM) containing 10 % Fetal bovine serum (FBS) at 37 °C under 5 % CO₂ in a humidified incubator. Following the harvesting of cells, the MCF-7 cells were counted (1×10⁴ cells/well) and transferred to a 96-well sterile microtiter plate in triplicates and incubated for another 24 h for proper adherence. When the cell growth reaches to 90 % confluency, the processed EC-SnHPO₄ composite in various concentrations of 25-250 µg/ml were treated to the cells and then incubated for another 24 h. The cells incubated with 25 µL of phosphate buffered saline (PBS) and no EC-SnHPO₄ treatment was used as control. Following the incubation period, the culture media was removed and replaced with a solution containing 175 µL of fresh medium and 25 µL of MTT (3-[4,5-dimethylthiazol-2-yl]-2,5-diphenyltetrazolium bromide) reagent and then incubated for another 4 h at 37 °C under 5 % CO₂. At the

completion of incubation period, the medium was replaced with a 100 µL of dimethyl sulfoxide to solubilize the formazan crystals formed as part of the cell's reaction with MTT reagent. The optical density was taken at an excitation wavelength of 575 nm and the results expressed are the percentage proliferation with respect to vehicle-treated cells. The values shown are the mean ± SD of three individual experiments.

Results and discussion

UV-visible spectroscopy

The absorption spectrum of EC-SnHPO₄ is shown in **Fig. 1** and the peak was recorded in the middle ultraviolet region of 200-300 nm. From the figure, the absorption maximum for the EC-SnHPO₄ composite observed to be around 287 nm. This absorption maximum can be attributed to the $\pi - \pi^*$ transition of the small electronic conjugated domains, i.e. aromatic C-C ring was found at the absorption peak of 287 nm [29].

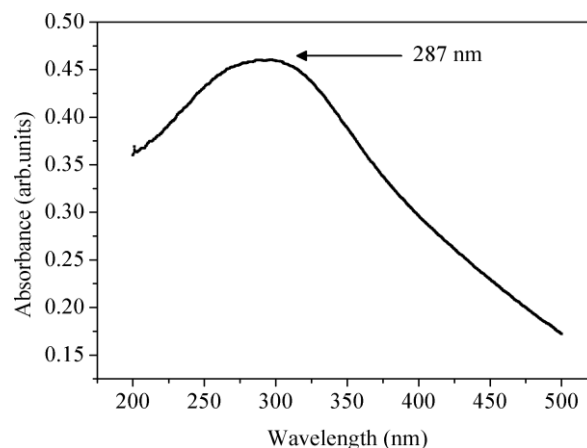


Fig. 1. UV-Vis absorption spectrum of the EC-SnHPO₄ composite.

By adjusting the Gaussian function such as,

$$y = y_0 + \left[\frac{A}{w\sqrt{\pi/2}} \right] \exp \left[-2(x - x_c)^2 / w^2 \right]$$

where, x and y denotes the wavelength and absorbance, respectively, the absorption spectra was synthesized. **Table 1** show the results of the Gaussian analysis for the system which was taken into account. The wavelength of the absorption which is found to be maxima ($\lambda_{max}=x_c$) and the corresponding transition energy ($h\nu$) in concise form is shown in **Table 1**.

Table 1. Gaussian curve analysis for the band in spectrum of EC-SnHPO₄ at 25°C.

System	Area of the curve (A)	Width of the curve (w)	Centre of the curve (x _c)	y ₀	R ²
EC-SnHPO ₄	44.289 ± 1.522	32.122 ± 0.736	224.220 ± 0.193	0.410 ± 0.018	0.97

Determination of ionization potential (I_D)

By employing the empirical equation that is generally derived from eminent personality such as Aloisi and

Pignataro, the ionization potential of the EC-SnHPO₄ was determined [30]:

$$I_D (eV) = 5.76 + 1.53 \times 10^{-4} \nu \quad (1)$$

where, ν is the wave number in cm⁻¹ of the EC-SnHPO₄. The ionization potentials determined for the EC-SnHPO₄ composite are also tabulated in **Table 2**.

Table 2. Various parameters like I_D , f , μ_{EN} , R_N and E for the EC-SnHPO₄ at 25°C.

System	λ (nm)	$h\nu$ (eV)	I_D (eV)	$f \times 10^5$	μ_{EN} (Debyes)	R_N (eV)	E (nm)
EC-SnHPO ₄	287	5.39	11.09	0.014	0.0115	3.243	4.333

Determination of oscillator strength (f)

The oscillator strength (f), which specifically has the dimensionless quantity employed are responsible for communicating the transition probability of the bands of the respective sample [31]. The extraction of the oscillator strength was also done from the absorption spectra and the following formula was used for the determination of the oscillator strength f :

$$f = 4.32 \times 10^{-9} \int \varepsilon \cdot d\nu \quad (2)$$

where, $\int \varepsilon \cdot d\nu$ is the area under the curve of the extinction coefficient of the absorption band in question vs. frequency. For first approximation, it is generally taken as:

$$f = 4.32 \times 10^{-9} \varepsilon \Delta\nu_{1/2} \quad (3)$$

where, ε is the maximum extinction coefficient on the band and $\Delta\nu_{1/2}$ is the half-width, i.e. the width of the band at half the maximum extinction. The observed oscillator strength of the band is summarized in **Table 2**.

Determination of transition dipole moment (μ_{EN})

The extinction coefficient is in aptitude relation with the transition dipole which is represented in the equation below:

$$\mu_{EN} = 0.0952 \left[\varepsilon \frac{\Delta\nu_{1/2}}{\Delta\nu} \right]^{1/2} \quad (4)$$

where, $\Delta\nu \approx \nu$ at ε and μ_{EN} is defined as $-e \int \psi_{ex} \sum_i r_i \psi_g d\tau$ and μ_{EN} for EC-SnHPO₄ is given in **Table 2** which is quite comprehensive as seen above.

Determination of resonance energy (R_N)

Briegleb and Czekalla [32] have theoretically derived the equation shown below:

$$\varepsilon = \frac{7.7 \times 10^{-4}}{h\nu/[R_N] - 3.5} \quad (5)$$

where, ε is the molar extinction coefficient of the material having the maximum range of the absorption, ν is the frequency of the peak and R_N is the resonance energy of the material in the ground state, which is responsible for contributing factor such as the stability constant of the material with a ground state property and is very prominent. The value of R_N of the material studied for EC-SnHPO₄ composite is also given in **Table 2**.

Determination of transition energy (E)

The transfer of lone pair of electrons was generally formed because of the hydrogen bond between the molecules which was presented by the existence of the new band in the material and the energy is calculated by employing the equation given by Briegleb [33].

$$E = \frac{1243.667}{\lambda} \text{ nm} \quad (6)$$

where, λ is the wavelength of the band of material and the data is shown in **Table 2**.

FTIR study

The FTIR spectra are responsible for the presence of functional groups which was determined by the brief study in **Fig. 2**. From the figure, the distinct peaks at 2960, 1435 and 1395 cm⁻¹ corresponds to the -CH stretching, -CH₃ and -CH₂ bending vibrations respectively from the EC groups [34]. The strong peak observed around 1076 cm⁻¹ corresponds to the C-O-C stretching in the cyclic ether of EC [35]. Similarly, the bands at 890, 780 and 507 cm⁻¹ are aspect for the vibration of PO₄³⁻ [36]. The grouping of sharp peaks at the region of 599 cm⁻¹ is characterised to the superposition of metal-oxygen stretching vibration and the peak in the region 1017 cm⁻¹ is generally due to the presence of HPO₄²⁻ [36-37]. The results of the study provided the proof for the covalent interaction that is taking place between EC and SnHPO₄.

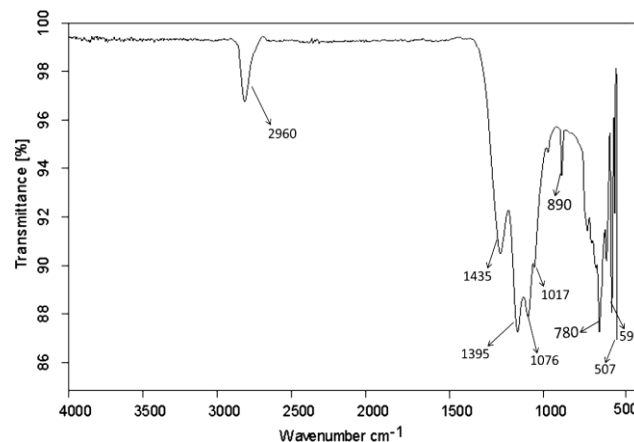


Fig. 2. FTIR spectrum of the EC-SnHPO₄ composite.

Conductivity study

In general, the conductivity of a solution does not change linearly with concentration. By plotting material

conductivity values against the square root of concentration, the effect of concentration on material conductivity can be studied in brief. It was found that variation of material conductivity with \sqrt{C} is dependent on the nature of electrolyte where **Table 3** is showing the behaviour of strong electrolytes with the change of concentration for the EC-SnHPO₄ composite. The variation is described in the form of obstruction of the polymer matrix that showed an increased variation as the diffusion pathway is on the way of resembling more tortuous and fractional pore volume showing a decreased variation [21].

The electrolytes such as KCl and NaCl are completely ionised at all range of concentrations or dilutions. It clearly indicates that the increase in the number of current carrying species is not responsible for the increase in material conductivity but it is basically because of the decrease in force of attraction between the ions of opposite charges with the decrease in concentration or increase in dilution. The forces of attraction between the opposite ions increase i.e. $(F \propto q_1 q_2 / r^2)$ at the higher concentration range and such phenomenon is called ionic interference. The conductivity is said to increase as the solution becomes more and more dilute.

The EC-SnHPO₄ composite material conductivity for 1:1 electrolyte solution was decreasing in the order $K^+ > Na^+$, in relation to the decrease in size of the cation which was mentioned by Beg *et al.* [38].

The temperature dependence of conductivity was adapted from the Arrhenius equation [39]:

Table 3. Material conductivity vs. concentration for the EC-SnHPO₄ using 1:1 electrolytes at $25 \pm 0.1^\circ\text{C}$.

Concentration (mole/l)	KCl (mS cm ⁻¹)	NaCl (mS cm ⁻¹)
0.5	4.47	3.49
0.1	6.11	428
0.07	10.59	5.52
0.05	13.98	6.82
0.02	17.8	13.08
0.01	18.2	13.5

$$\Lambda = \frac{P}{T} \exp\left(\frac{-E_a}{RT}\right) \quad \text{----- (7)}$$

where, P is constant and known as Arrhenius factor. It is also called pre-exponential factor. E_a is the activation energy. The factor $\exp\left(\frac{-E_a}{RT}\right)$ is generally corresponding to

the fraction of molecules which have energy greater than E_a , T is the absolute temperature and R is the gas constant.

Eq. (7) may be written as given below:

$$\log \Lambda T = \log P - \frac{E_a}{2.303RT} \quad \text{----- (8)}$$

It is clearly visible and resembling from the equation that as the value of activation energy, E_a increases, the value of ΛT decreases.

The activation energy is now calculated from Eq. (8). When $\log \Lambda T$ is plotted against $1/T$, a straight line is formed

as shown in **Fig. 3**. From the figure, the intercept of the straight line is equal to $\log P$ and slope is equal to $\frac{E_a}{2.303R}$.

Fig. 3 shows the increase in conductivity with an increase of temperature. When the temperature zone is overviewed, the sample shows the linear pathway which makes it clear that the graph plotted is approximately parallel to temperature axis resembling that the conductivity is independent of lower temperatures [40]. The values of conductivity lie in the order of 10^{-3} Scm^{-1} , showing that the EC-SnHPO₄ composite is falling along the semi-conductor region [41].

The band gap is defined as the minimum amount of energy that is required for an electron to break the bound state freely. The electron is excited into a free state only when the band gap matches with the excitation energy and finally the material participates into conduction. A hole is generated at the region of the electron bounding and the hole also participates in conduction. One of the important optical properties of inorganic semiconductors is represented as below [39]:

$$\Lambda = \frac{P}{T} \exp\left(\frac{-E_g}{2kT}\right) \quad \text{----- (9)}$$

As all the possible distribution of electrons in the conduction band is independent of the distribution of holes in the valence band, the factor of $\frac{1}{2}$ in the exponent is found to locate with the inorganic semiconductor.

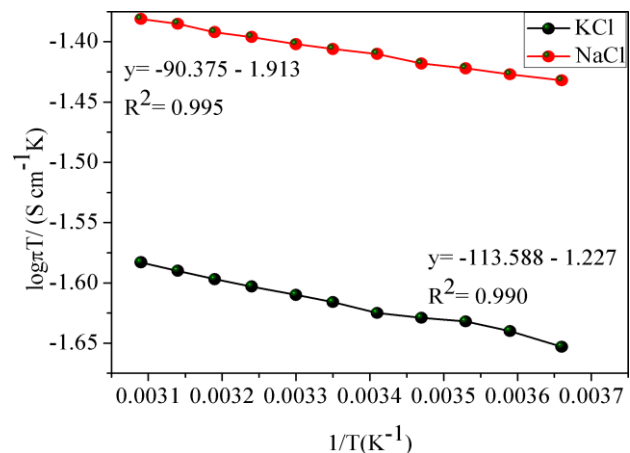


Fig. 3. Plot of material conductivity vs. temperature for the EC-SnHPO₄ using 0.5 M of 1:1 electrolytes at $(25-50) \pm 0.1^\circ\text{C}$.

From the Eqs. (7) and (9), we get the respective equation:

$$E_a = \frac{E_g}{2} \quad \text{----- (10)}$$

So we can notice that the conductivity is thermally activated to attain its activation energy which is half the band gap.

The activation energy (eV) for 1:1 electrolyte solution was randomly estimated from the slope of Arrhenius plots by using linear regression method which is in accordance with the equation given above and is shown in the **Table 4**.

From the table, it was detected that the activation energy is in relation with the electro-negativity of the metal ions and is found to be dependent on each other. With a decrease of the electro-negativity of metal ion, the activation energy found to be increased.

Table 4. Activation and band gap energies of conduction for the EC-SnHPO₄ when used 0.5 M of 1:1 electrolytes at (25-50) ± 0.1 °C.

Electrolyte (mol L ⁻¹)	Activation energy (eV)	Band energy gap (eV)
KCl	0.022	0.044
NaCl	0.017	0.034

The variation of the activation energy with the EC-SnHPO₄ and various electrolytes of 1:1 concentration at room temperature is shown in the **Fig. 4**. From the figure, it clearly states that the activation energy depends on the electrolyte concentration and increases with an increase in the concentration due to the nature of the solvent and for that different electrolyte at a particular concentration, where K⁺>Na⁺ are equivalent to the order of crystallographic radii of the alkali metal cations. The motion of penetrating species is governed by the segmental mobility of the polymer when it moves in as polymer substance which contain relatively small amount of water where the diffusiveness is dependent on the probability of the segment making large hole to accommodate a penetrate species in its respective surrounding [42].

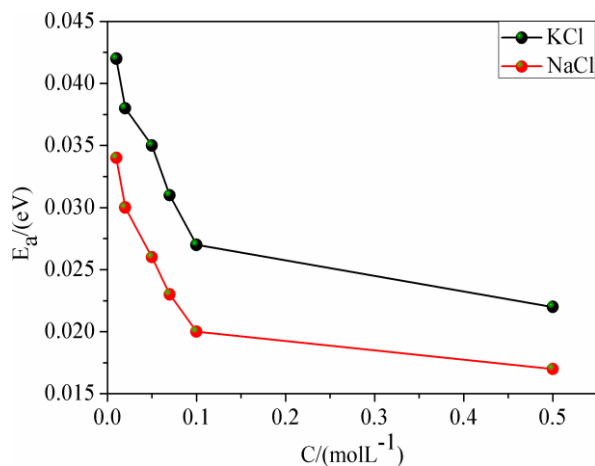


Fig. 4. Plot of activation energy vs. concentration for the EC-SnHPO₄ using 1:1 electrolytes at 25±0.1°C.

pH study

The pH response profile for the EC-SnHPO₄ was tested by using the 1 × 10⁻² mol L⁻¹ electrolyte solution on the pH range 1.0 – 12.0. The pH of the solution was maintained by inducing small drops of hydrochloric acid (0.1 M) or sodium hydroxide (0.1 M) into the solutions where the **Fig. 5** is showing the influence of the pH response on the composite EC-SnHPO₄ electrode. As the figure clearly states that the potential is constant from pH 4.0 to 7.5 and after that, the drifts in the potentials are noticed due to the formation of some hydroxyl complexes of cations in the solution. At lower pH, the potentials are increased and resembled that the membrane responded well to protonium ions, as a result of some extent of protonation of phosphorus atoms of the phosphate group. On the other

hand at lower pH values, the H₃O⁺ ions was contributing highly to the charge transport process by the EC-SnHPO₄ which was the basic cause of interference [43].

Antibacterial study

The EC-SnHPO₄ composite was tested for its antibacterial activity by making use of the disk diffusion method [27, 28] against two different bacteria of a gram positive, *Staphylococcus aureus* (MSSA-22) and the gram negative bacteria of *Escherichia coli* (K-12). Tetracycline drug was used as the positive standard for the comparison of antibacterial property of EC-SnHPO₄ and **Table 5** shows the results which are quite specific to each bacteria. From the analysis of results, an extraordinary inhibitory effect in response to the growth of the bacterial strains was observed on treatment of the EC-SnHPO₄ composite (100 µg/ml). Also, the comparison of data given in the table indicates that the EC-SnHPO₄ resembles more activity against *Staphylococcus aureus* when compared to the *Escherichia coli*. That too on comparison with Tetracycline drug, the antibacterial activity of EC-SnHPO₄ is higher against both the bacterial strains and this can be due to the presence of Sn metal. Also, the presence of EC led for higher interaction of the composite with the bacterial strains and thus inhibition of bacterial growth. This is supported by a similar study where the researchers have investigated the antimicrobial property of 1,6-bis(benzimidazol-2-yl)-3,4-dithiahexane ligand complexed with Hg(II) and was found that the activity is mostly due to the increased interaction of the ligand with the bacterial cells [44]. The results of the study therefore confirming the antibacterial behaviour of EC-SnHPO₄ composite.

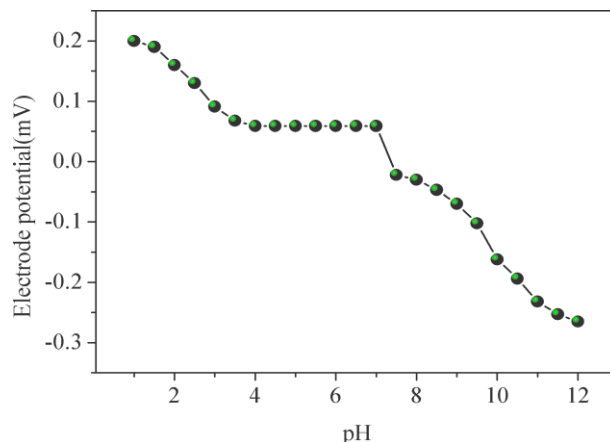


Fig. 5. Effect of pH of the KCl solutions (1 × 10⁻² mol L⁻¹) on the potential response of the EC-SnHPO₄.

Table 5. Antibacterial activity of EC-SnHPO₄ (100 µg/ml).

Bacteria	Diameter of zone of inhibition (mm)	
	EC-SnHPO ₄	Tetracycline
<i>Staphylococcus aureus</i>	15.4 ± 0.25	9.3 ± 0.85
<i>Escherichia coli</i>	12.6 ± 0.15	9.7 ± 0.20

Anticancer effect

The anticancer effect of the EC-SnHPO₄ composite (25-250 µg/ml) towards MCF-7 breast cancer cell line for a 24 h incubation period is shown in the **Fig. 6**. From the

figure, it can be seen clearly that a concentration dependent decrease in the number of MCF-7 cancer cells is observed. A decrease close to 60 % is observed for the 100 $\mu\text{g/ml}$ concentration of EC-SnHPO₄ and further increase of concentration to 150, 200 and 250 $\mu\text{g/ml}$ led for the decrease in the number of cells to 50, 41 and 28 % respectively. This decrease in the proliferation of cancer cells towards the treatment of EC-SnHPO₄ composite may be due to the toxic behaviour exhibited by the Sn metal, as EC serves as the vehicle for an increased interaction of the composite with the cell. The Sn metal with its electron deficient nature (+2) can easily grab the electrons from the electron rich intracellular protein components. This further led to the generation of reactive free radicals that can be responsible for many of the intracellular reactions and inhibits the proliferation of cells. The inhibition of cancer cell growth therefore, confirming the anticancer behaviour of the EC-SnHPO₄ composite.

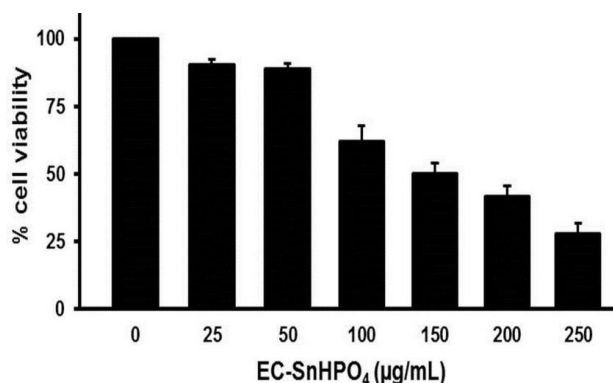


Fig. 6. Comparison of the anticancer effect of EC-SnHPO₄ composite towards MCF-7 breast cancer cells.

Conclusion

In conclusion, we provide the synthesis, characterization, antibacterial and anticancer behaviour of a quite stable EC-SnHPO₄ composite material that was prepared by the sol-gel method. The physico-chemical characterization of the composite material was established by UV-Vis and FTIR studies. The material conductivities were measured across the EC-SnHPO₄ composite by disintegrating different electrolytes (1:1) at various ranges of concentration and temperatures. The different parameters such as ionization potential (I_D), oscillator strength (f), transition dipole moment (μ_{EN}), resonance energy (R_N), and transition energy (E) were investigated for the EC-SnHPO₄ composite. The cross-linked rigid framework of EC provided adequate adhesion to the EC-SnHPO₄ composite, in addition to be responsible for the higher mechanical stability. The antibacterial study of composite material was able to show some good results against two different bacteria than the tetracycline drug, and can potentially be used as antibacterial agent. The reduced proliferation of cancer cells on treatment of the composite providing the information that the composite can also be used an ingredient in cancer therapeutic drugs.

Acknowledgements

FM would like to thank the School of Pharmacy, NorthWest University, Potchefstroom, South Africa for providing the facility to characterize the material and also Universiti Putra Malaysia for the funding.

Reference

- (a). Arfin, T.; Yadav, N. J; *Ind. Eng. Chem.*, **2013**, *19*, 256. DOI: [10.1016/j.jiec.2012.08.009](https://doi.org/10.1016/j.jiec.2012.08.009)
(b). Mohammad, F.; Arfin, T; *Bull. Environ. Contam. Tox.*, **2013**, *91*, 689. DOI: [10.1007/s00128-013-1131-3](https://doi.org/10.1007/s00128-013-1131-3)
- Arfin, T.; Falch, A.; Kriek, R.J; *Phys. Chem. Chem. Phys.*, **2012**, *14*, 16760. DOI: [10.1039/c2cp42683h](https://doi.org/10.1039/c2cp42683h)
- (a). Mohammad, F.; Arfin, T; *Adv. Mat. Lett.*, **2014**, *5*, 315. DOI: [10.5185/amlett.2014.amwc.1030](https://doi.org/10.5185/amlett.2014.amwc.1030)
(b). Khan, A.A.; Baig, U. J; *Ind. Eng. Chem.*, **2012**, *18*, 1937. DOI: [10.1016/j.jiec.2012.05.008](https://doi.org/10.1016/j.jiec.2012.05.008)
- (a). Nabi, S.A.; Naushad, M; *Colloids Surf. Part A: Physicochem. Eng. Aspects*, **2008**, *316*, 217. DOI: [10.1016/j.colsurfa.2007.09.005](https://doi.org/10.1016/j.colsurfa.2007.09.005)
(b). Kumar, A.P.; Depan, D.; Tomer, N.S. Singh, R.P; *Prog. Polym. Sci.* **2009**, *34*, 479. DOI: [10.1016/j.progpolymsci.2009.01.002](https://doi.org/10.1016/j.progpolymsci.2009.01.002)
- Parikh, N.H.; Porter, S.C.; Rohera, B.D; *Pharm. Res.*, **1993**, *10*, 525. DOI: [10.1023/A:1018989717297](https://doi.org/10.1023/A:1018989717297)
- Lin, W.J.; Wu, T.L; *J. Microencapsulation*, **1999**, *16*, 639. DOI: [10.1080/026520499288825](https://doi.org/10.1080/026520499288825)
- Crowley, M.M.; Schroeder, B.; Fredersdorf, A.; Obara, S.; Talarico, M.; Kucera, M.; McGinity, J.W; *Int. J. Pharm.* **2004**, *269*, 509. DOI: [10.1016/j.ijpharm.2003.09.037](https://doi.org/10.1016/j.ijpharm.2003.09.037)
- (a). Bruno, L.; Kasapis, S.; Chaudhary, V.; Chow, K.T.; Heng, P.W.S.; Leong, L.P; *Carbohydr. Polym.*, **2011**, *86*, 644. DOI: [10.1016/j.carbpol.2011.05.002](https://doi.org/10.1016/j.carbpol.2011.05.002)
(b). Appel, L.E.; Zentner, G.M; *Pharm. Res.*, **1991**, *8*, 600. DOI: [10.1023/A:1015800606298](https://doi.org/10.1023/A:1015800606298)
- Nelson, K.G.; Bainbridge, C.A; *J. Dental Res.*, **1973**, *52*, 318. DOI: [10.1177/00220345730520022101](https://doi.org/10.1177/00220345730520022101)
- Yellin, W.; Cilley, W.A; *Spectrochim Acta Part A: Mol. Spectrosc.*, **1969**, *25*, 879. DOI: [10.1016/0584-8539\(69\)80059-0](https://doi.org/10.1016/0584-8539(69)80059-0)
- Klement, R.; Haselbeck; *Eur. J. Inorg. Chem.*, **1963**, *96*, 1022. DOI: [10.1002/cber.19630960416](https://doi.org/10.1002/cber.19630960416)
- Berndt, A.F.; Lamberg, R; *Acta Crystallogr Sect. A: Fundam. Crystallogr.*, **1971**, *27*, 1092. DOI: [10.1107/S0567740871003571](https://doi.org/10.1107/S0567740871003571)
- Gillespie, R.J.; Nyholm, R.S.; *Q. Rev. Chem. Soc.*, **1957**, *11*, 339. DOI: [10.1039/QR9571100339](https://doi.org/10.1039/QR9571100339)
- Donaldson, J.D; *Prog. Inorg. Chem.*, **1967**, *8*, 287. DOI: [10.1002/9780470166093.ch5](https://doi.org/10.1002/9780470166093.ch5)
- Cilley, W.A; *Inorg. Chem.*, **1968**, *7*, 612.
- Gnusin, N.P.; Zabolotsky, V.I.; Nikonenko, V.V.; Urtenov, M.R; *Elektrochim.*, **1986**, *22*, 298.
- Zabolotsky, V.I.; Nikonenko, V.V; *J. Membr. Sci.* **1993**, *79*, 181.
- Chaabane, L.; Dammak, L.; Nikonenko, V.V.; Bulvetre, G.; Auclair, B.J; *J. Membr. Sci.*, **2007**, *298*, 126. DOI: [10.1016/j.memsci.2007.04.010](https://doi.org/10.1016/j.memsci.2007.04.010)
- Choi, J.H.; Kim, S.H.; Moon, S.H; *J. Colloid Interface Sci.*, **2001**, *241*, 120. DOI: [10.1006/jcis.2001.7710](https://doi.org/10.1006/jcis.2001.7710)
- Arfin, T.; Fatima S; *Asian J. Adv. Basic Sci.*, **2014**, *2*, 14.
- Arfin, T.; Rafiuddin; *Desalination*, **2012**, *284*, 100. DOI: [10.1016/j.desal.2011.08.042](https://doi.org/10.1016/j.desal.2011.08.042)
- Arfin, T.; Jabeen, F.; Kriek, R.J; *Desalination*, **2011**, *274*, 206. DOI: [10.1016/j.desal.2011.02.014](https://doi.org/10.1016/j.desal.2011.02.014)
- Arfin, T.; Rafiuddin; *Electrochim. Acta*, **2009**, *54*, 6928. DOI: [10.1016/j.electacta.2009.06.074](https://doi.org/10.1016/j.electacta.2009.06.074)
- Arfin, T.; Rafiuddin; *Electrochim. Acta*, **2010**, *55*, 8628. DOI: [10.1016/j.electacta.2010.07.091](https://doi.org/10.1016/j.electacta.2010.07.091)
- (a). Arfin, T.; Rafiuddin; *Electrochim. Acta*, **2011**, *56*, 7476. DOI: [10.1016/j.electacta.2011.06.109](https://doi.org/10.1016/j.electacta.2011.06.109)
(b). Arfin, T.; Yadav, N; *Anal. Bioanal. Electrochem.*, **2012**, *4*, 135.
- Arfin, T.; Bushra, R.; Kriek, R.J; *Anal. Bioanal. Electrochem.* **2013**, *5*, 206.
- Cruickshank, R.; Duguid, J.P.; Marmion, B.P.; Awain, R.H.A; *Medicinal Microbiology*; 12th ed., Churchill Livingstone: London, **1997**, Vol. 11, pp 196.
- Collins, A.H; *Microbiology Method*; 2nd ed., Butterworth: London, **1976**.
- Kalsi P.S; *Spectroscopy of organic compounds*; 6th ed., New Age International Publishers: New Delhi, **2009**.

30. Aloisi, G.G.; Pignataro, S; *J. Chem. Soc. Faraday Trans.* **1973**, *69*, 534.
DOI: [10.1039/F19736900534](https://doi.org/10.1039/F19736900534)
31. Lever, A.B.P.; *Inorganic Electronic Spectroscopy*; 2nd ed., Elsevier: Amsterdam; **1985**; pp 161.
DOI: [10.1016/0022-2860\(85\)80208-8](https://doi.org/10.1016/0022-2860(85)80208-8)
32. Briegelab, G.; Czekalla J; *Z. Phys. Chem.* **1960**, *24*, 37.
DOI: [10.1524/zpch.1960.24.1_2.037](https://doi.org/10.1524/zpch.1960.24.1_2.037)
33. Briegleb, G; *Angew. Chem.*, **1964**, *76*, 326.
DOI: [10.1002/ange.19640760804](https://doi.org/10.1002/ange.19640760804)
34. Desai, J.; Alexander K.; Riga, A; *Int. J. Pharm.*, **2006**, *308*, 115.
DOI: [10.1016/j.ijpharm.2005.10.034](https://doi.org/10.1016/j.ijpharm.2005.10.034)
35. Bai, Y.; Jiang, C.; Wang, Q.; Wang, T; *Carbohydr. Polym.*, **2013**, *96*, 522.
DOI: [10.1016/j.carbpol.2013.04.026](https://doi.org/10.1016/j.carbpol.2013.04.026)
36. Rao, C.N.R; *Chemical Applications of Infrared Spectroscopy*; Academic Press: New York, **1963**; pp 338.
37. Nabi, S.A.; Bushra, R.; Naushad, M.; Khan, A.M; *Chem. Eng. J.* **2010**, *165*, 529.
DOI: [10.1016/j.cej.2010.09.064](https://doi.org/10.1016/j.cej.2010.09.064)
38. Beg, M.N.; Ahmad, K.; Altaf, I.; Arshad, M; *J. Membr. Sci.*, **1981**, *9*, 303.
DOI: [10.1016/S0376-7388\(00\)80271-9](https://doi.org/10.1016/S0376-7388(00)80271-9)
39. Arfin, T.; Mohammad, F; *J. Ind. Eng. Chem.*, **2013**, *19*, 2046.
DOI: [10.1016/j.jiec.2013.03.019](https://doi.org/10.1016/j.jiec.2013.03.019)
40. Onwudiwe, D.C.; Arfin, T.; Atrydom, C.A.; Kriek, R.J; *Electrochim. Acta*, **2013**, *109*, 809.
DOI: [10.1016/j.electacta.2013.07.176](https://doi.org/10.1016/j.electacta.2013.07.176)
41. Nalwa, H.S; *Handbook of advanced lectronic and photonic materials and devices*; Academic Press: New York, **2001**.
DOI: [10.1016/B978-012513745-4/50000-7](https://doi.org/10.1016/B978-012513745-4/50000-7)
42. Cumins, C.A.; Kwei, T.K; *In Diffusion in polymers*; Crank, J.; Park, G.S., Eds.; Academic Press: London, **1968**.
43. Arfin, T.; Kumar, C; *Anal. Bioanal. Electrochem.* **2014**, *6*, 403.
44. Aghatabay, N.M.; Tulu, M.; Mahmiani, Y.; Somer, M.; Dulger, B; *Struct. Chem.*, **2008**, *19*, 71.
DOI: [10.1007/s11224-007-9253-z](https://doi.org/10.1007/s11224-007-9253-z)

Advanced Materials Letters

Copyright © VBRI Press AB, Sweden

www.vbripress.com

Publish your article in this journal

Advanced Materials Letters is an official international journal of International Association of Advanced Materials (IAAM, www.iaamonline.org) published by VBRI Press AB, Sweden monthly. The journal is intended to provide top-quality peer-review articles in the fascinating field of materials science and technology particularly in the area of structure, synthesis and processing, characterisation, advanced-state properties, and application of materials. All published articles are indexed in various databases and are available download for free. The manuscript management system is completely electronic and has fast and fair peer-review process. The journal includes review article, research article, notes, letter to editor and short communications.

